

Modeling surveillance and interventions in the 2014 Ebola epidemic

Marisa C. Eisenberg^{†‡}, Joseph N.S. Eisenberg[†], Jeremy P. D'Silva^{*†}, Eden V. Wells[†],
Sarah Cherng[†], Yu-Han Kao[†], and Rafael Meza[†]

[†] Department of Epidemiology, School of Public Health, University of Michigan, Ann Arbor

[‡] Department of Mathematics, University of Michigan, Ann Arbor

^{*} Father Gabriel Richard High School, Ann Arbor

Abstract

The 2014 Ebola epidemic in West Africa is the largest ever recorded, and understanding the interrelated dynamics of surveillance and intervention is a key concern, both for this and future epidemics. Moreover, as transmissibility and mortality are believed to increase as symptoms progress, intervention strategies may depend on individual's stage of infection. To examine these issues, we developed a stage-structured model of Ebola, which includes a term for fraction of the population at risk, reporting rate, among other factors. We generated short term forecasts for Guinea, Liberia, and Sierra Leone, beginning October 1, 2014, which we have since validated using subsequent data. We examined the relative contributions of the stages of infection, and then expanded the model to consider Ebola treatment unit (ETU) dynamics and interventions, incorporating both stage-dependent hospitalization rates and dynamic ETU capacity.

We found that a wide range of forecasted trajectories fit well to the data. However, by estimating terms for surveillance and intervention, the best-fit models correctly forecasted the qualitative behavior for all three countries, both individually and for all countries combined. In particular, the models correctly forecasted the slow-down and stabilization in Liberia but continued exponential growth in Sierra Leone through October and November 2014. Because increasing intervention levels lead to improved reporting, interventions and reported cases/deaths can have a seemingly paradoxical relationship, in which increasing intervention levels result in apparent increases in cases and deaths (due to improved reporting), even though there has actually been a significant reduction in underlying total cases/deaths. These simulations suggest that some of the observed reductions in the growth rate of the epidemic are consistent with intervention effects. All three transmitting stages (early, late, and funeral) appeared to contribute significantly to transmission, with intervention on any single stage often insufficient to prevent an epidemic. However, parameter unidentifiability issues impede estimation of the relative contributions of each stage of transmission from incidence and deaths data alone, which poses a challenge in determining optimal intervention strategies, and underscores the need for additional data collection. For the ETU-based scenarios, basic treatment and isolation capacity acted as a prerequisite to other interventions, with early-stage isolation, increased staff and supplies, and reductions in funeral transmission only fully effective once sufficient ETU/isolation capacity was achieved.

1 Introduction

The ongoing 2014 Ebola outbreak is unprecedented in both its size and complexity, dwarfing the numbers of cases and deaths for all previous outbreaks combined [1]. The outbreak began in Guinea on March 23, 2014 [1], and has since spread to yield widespread and intense transmission in Guinea, Liberia, and Sierra Leone, as well as cases in five additional countries (Nigeria, Senegal, Mali, Spain, USA), with over 17,000 cases reported as of December 2014 [2]. Intervention efforts have increased over the months following, although the epidemic spread continues.

Ebola virus disease (EVD) was first identified in 1976, in two simultaneous outbreaks in Sudan and the Democratic Republic of the Congo [3]. It is not completely understood why this epidemic has expanded to such an unprecedented scale compared to previous outbreaks, although regional instability, urbanization, and lack of capacity have all been suggested as potential factors [4]. EVD is transmitted by contact with body fluids [3, 5]. Healthcare workers are at particular risk for transmission due to their frequent contact with patients and body fluids, and burial ceremonies in which mourners contact the body of the deceased have also been identified as playing an important role in transmission [3, 5, 6]. Ebola has an average incubation period of 8-10 days (with a range of 2-21 days), and infectiousness is believed to coincide with symptom onset [3]. EVD progresses in two broad stages [3, 7]. Symptoms in the first stage often include fever, headache, sore throat, fatigue, and muscle pain, and the first stage can often be mistaken for other diseases, such as malaria or typhoid [3]. This is sometimes followed by a brief pseudo-recovery [7], and then a second stage which includes more intense symptoms such as vomiting, diarrhea, rash, symptoms of impaired kidney and liver function, and in some cases internal and external bleeding [3, 8]. Recovery is more likely from the first stage, with much higher death rates in the second stage (indeed, in some outbreaks all second-stage patients died [7]). As second stage symptoms tend to have more release of body fluids (e.g. vomit or diarrhea), transmissibility is likely to be higher as the disease progresses as well. Accounting for the stage structure is thus particularly important when evaluating healthcare capacity and how the timing of hospitalization may affect the outbreak dynamics.

Surveillance in the current epidemic has presented challenges, with ongoing changes in reporting as the outbreak continues [2]. Reporting rate estimates are difficult, although some have been presented [9]. Additionally, the fraction of the population at risk and the level of asymptomatic infection and preexisting immunity are largely unknown for the current outbreak. The potential for existing immunity and asymptomatic infection have been noted as a potentially key factor which can lead to overestimation of incidence when forecasting [10]. Changing Ebola treatment unit (ETU) capacity and interventions can also alter both the reporting rate and the effective fraction of the population at risk, adding another facet to this complex issue.

Intervention efforts have been ongoing with increasing intensity since the beginning of the outbreak, although in some regions the epidemic continues to spread, with steady or increasing numbers of weekly cases in Guinea and Sierra Leone [2]. Recent and ongoing efforts include increasing ETU capacity and numbers of ETUs, additional staff and supplies, burial teams, and efforts to increase trust and build community relationships [2, 11–14]. Additionally, in some regions, efforts have been made to reduce individual mobility and border crossings [15, 16], and some areas have provided home health kits containing gloves, gowns, disinfectants, and other supplies to help caretakers at home reduce the potential for transmission [17, 18]. Ongoing vaccine developments provide a potential new avenue for intervention and are currently in development and clinical trials [19].

There have been a wide range of simulation models developed for EVD in recent months [9, 10, 20–29], many of which are based on early models by Chowell, Llegend, and others [30–32]. Several models have been used for forecasting and understanding disease dynamics [9, 10, 20, 22], disease progression and immunity [10, 29], and evaluating the potential effects of alternate interventions [23, 33].

In this paper, we develop a stage-structured model of Ebola transmission which explicitly incorporates the natural history of the disease and the dynamics of ETU capacity, as well as considering issues such as reporting rates, symptomatic fraction, and fraction of the population at risk. We use this model to evaluate the uncertainty in forecasts of cases, deaths, and beds needed, estimate the contributions of each stage of illness to transmission, as well as to examine how the timing of interventions in ETU capacity, staff/supplies, case-finding, and funeral transmission reduction affect the EVD outbreak dynamics.

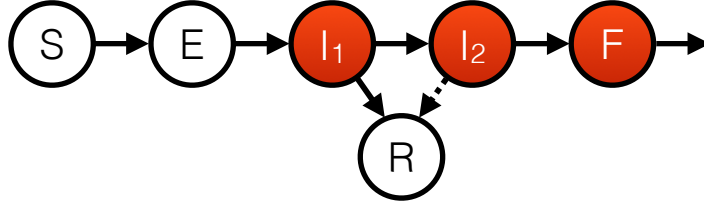


Figure 1: Stage-structured compartmental model of Ebola transmission. Red compartments are transmissible, and recovery rates are greater from I_1 than from I_2 [7].

2 Data

We examined data on incidence of suspected cases and deaths from Guinea, Liberia, Sierra Leone, and all countries combined, as reported by the World Health Organization (WHO) [2]. For estimating the model parameters, we used start dates for each country roughly corresponding to when each location began consistent exponential growth, to avoid issues due to initial stochasticity and hurdles in setting-up reporting systems (e.g. some early data shows decreases in cumulative cases, likely due to changes in surveillance systems, case definitions, etc.). Ongoing efforts to increase the response to the current epidemic have escalated particularly since October 1, for example with the beginning of the first-ever UN emergency health mission, the UN Mission for Ebola Emergency Response (UN-MEER) on October 1, 2014 [13]. Additionally, the data beginning in October has shown increased uncertainty and changes in reporting, with incomplete reporting data, and significant decreases in reported cumulative cases (likely due to changes in reporting) [2]. A recent WHO Roadmap update stated that “the capacity to capture a true picture of the situation in Liberia remains hamstrung by underreporting of cases” [34]. Thus, we fitted data up through October 1, 2014, with subsequent data used primarily for validation and exploring alternate intervention strategies, as described below.

3 Stage-Structured Model Simulations

3.1 Model Structure

We begin with the stage-structured compartmental model shown in Figure 1. The model incorporates a staged infection process to reflect the increasing symptoms and transmissibility as the infection progresses [3, 7]. As described above, Ebola often progresses through multiple stages of illness—an initial infectious stage in which symptoms tend to be milder (such as fever, headache, sore throat, muscle aches), often progressing to diarrhea, vomiting, and a second, more intense stage during which the more advanced symptoms (such as hemorrhaging and multi-organ failure) manifest [3, 7], with a typical time to progression of approximately 5-7 days [8]. Most recoveries occur from the first stage, while the second stage is typically fatal [7, 8, 35, 36]. Thus, we consider two stages of infection here (although one might consider an arbitrary number of stages to more

finely capture the progression of the illness). The corresponding equations for Figure 1 are:

$$\begin{aligned}
\frac{dS}{dt} &= -(\beta_I I_1 + \beta_2 I_2 + \beta_F F)S \\
\frac{dE}{dt} &= (\beta_I I_1 + \beta_2 I_2 + \beta_F F)S - \alpha E \\
\frac{dI_1}{dt} &= \alpha E - \gamma_1 I_1 \\
\frac{dI_2}{dt} &= \delta_1 \gamma_1 I_1 - \gamma_2 I_2 \\
\frac{dF}{dt} &= \delta_2 \gamma_2 I_2 - \gamma_F F \\
\frac{dR}{dt} &= (1 - \delta_1) \gamma_1 I_1 + (1 - \delta_2) \gamma_2 I_2 - \gamma_R R
\end{aligned} \tag{1}$$

where S represents the fraction of the population which is susceptible, E the fraction exposed, I_1 the fraction in the first stage of infection, I_2 the second stage of infection, R the fraction of the population which who are recently recovered (i.e. who would still require an ETU bed if hospitalized), and F the fraction of the population who have died and are in the process of being buried (as funerals provide an alternate route of transmission as in the models based on [31]).

We note that although recovered individuals have some chance of transmission for up to seven weeks after recovery (e.g. via semen or breast milk [35]), for simplicity we do not include the transmission in these later stages. For book-keeping purposes we track recently recovered (R), in order to estimate the total number of ETU beds needed over time. This does not affect the dynamics of infection since the recovered individuals are assumed to have full immunity and to be unable to transmit the virus. Because we consider only relatively short time frame here (< 1 year), for simplicity we ignore population background births and deaths. Lastly, we note that this simplified model lumps together both community and hospital/ETU infected.

The model structure is somewhat similar to the SEIHFR model of Legrand et al. [31], in which infected individuals in the community (I) can be admitted to the hospital (H), but the progression in this model is through the natural history of the disease rather than from household to hospital. Thus, there are different mechanistic assumptions underlying the two models, so that even though the resulting compartmental diagrams are similar, there are important differences in the flows between compartments. For example, SEIHFR models typically assume lower transmission in the ETU stage [23], which contrasts with the higher transmission rates in the second stage of infection used here; additionally, mortality is significantly higher for infected individuals in the community than in the hospital, where by contrast there is higher recovery in the first stage and death only after the second stage of infection in the model used here. In subsequent sections of this paper we also consider an expanded model that includes compartments for infected individuals admitted to an ETU, which allows us to capture both the stage structure and ETU dynamics.

Basic Reproduction Number. Using the second-generation matrix approach [37, 38], the basic reproduction number for the model is given by:

$$\mathcal{R}_0 = \frac{\beta_1}{\gamma_1} + \frac{\beta_2 \delta_1}{\gamma_2} + \frac{\beta_F \delta_1 \delta_2}{\gamma_F}. \tag{2}$$

where \mathcal{R}_0 for the system breaks into three portions based on each transmission stage, weighted by the fraction of individuals who reach that stage and the amount of time spent in each stage (as is typical for stage structured models [38]).

Measurement Equations. Lastly, to connect the model to the data on cumulative cases and deaths provided by the WHO, we append the following measurement equations to (1):

$$\begin{aligned} y_C &= kN \int_0^t \alpha E d\tau, \\ y_D &= kN \int_0^t \delta_2 \gamma_2 I_2 d\tau, \end{aligned} \tag{3}$$

where y_C represents cumulative cases, and y_D cumulative deaths. The parameter k represents a combination of several factors, including: the fraction of the population at risk (whether due to social contact structure, spatial heterogeneity, immunity from asymptomatic infection, or other factors), a rough correction for errors in our initial condition assumptions, as well as the reporting rate. Although in reality the reporting rate is likely to be different for cases and deaths, we found that the model fit well for a wide range of values for k (as described further below), so for simplicity we set the two to be equal.

3.2 Parameter Estimation Methods

Table 1 gives the parameter definitions, values, ranges, and sources. To more easily frame δ_1 in terms of known values, we let $\delta = \delta_1 \delta_2$ be the overall mortality rate (fraction) of infected individuals, and work using δ rather than δ_1 . For the total population size, N , we used a total population of 11,745,189 for Guinea, 4,294,077 for Liberia, and 6,092,075 for Sierra Leone, as determined by the World Bank [39].

We would expect there to be a wide range of model parameters that fit the data equally well—particularly as the data up through October 1 is still in the exponential growth phase, during which it can be fitted with only two parameters (i.e. as one would fit a line on a log scale). This idea has been used to develop simple two-parameter predictive models of the epidemic, such as [25], and explored more thoroughly in an identifiability context in [40]. This represents an inherent unidentifiability problem during this period of the epidemic, as a wide range of parameter values can be used to generate the same initial epidemic growth rate, but may have different points in time at which the epidemic dynamics begin to deviate from exponential growth. Thus, we used a Latin Hypercube (LH) sampling approach in which we sampled most of our parameters across realistic ranges given in Table 1, and then for each sample, we fit only two parameters, the transmission parameter β_1 and the overall mortality rate δ . This allows us to examine the range of potential model behaviors consistent with both the data and the known realistic ranges for all parameters. Since realistic values for k are largely unknown (as k accounts for a wide range of factors), the range for k was very broadly, with an upper bound of 1 (representing perfect reporting and a completely at-risk population) and an approximate lower bound determined by taking the lowest value which still yielded qualitatively good fits. We LH-sampled 1000 parameter sets for each case (all countries combined, Guinea, Liberia, and Sierra Leone). We also tested the extrema of each range in Table 1, to illustrate the full range of potential behaviors generated by the model in the realistic ranges.

To fit the model, we used least squares fitted to cumulative cases and deaths via the measurement equations (3), using Nelder-Mead optimization in MATLAB [41]. Cumulative incidence measurements such as those used here suffer from a lack of independence between measurements (as each subsequent measurement is clearly dependent on the previous), which has been noted to result in artificially small confidence bounds on parameter estimates and forecasts [42]. However, since there are different timings between case count reports, incident cases are somewhat more difficult to work with, and interpolating between case reports to generate regular incidence counts (e.g. daily) would also suffer from some degree of lack of independence, and making the cumulative

	Definition	Units	Range	Source
β_1	Transmission parameter for first stage of illness	people ⁻¹ days ⁻¹	Estimated	Estimated
$\frac{\beta_2}{\beta_1}$	Ratio of infectiveness in first vs. second stage of illness	unitless	1.5 - 5	[29, 43]
$\frac{\beta_F}{\beta_1}$	Ratio of infectiveness in first stage vs. funeral transmission	unitless	1.5 - 5	[23, 29, 43]
α^{-1}	Average incubation period	days	8-10	[3, 5]
γ_1^{-1}	Length of first stage of illness	days	5 - 7	[3, 7]
γ_2^{-1}	Length of second stage of illness	days	1 - 2	[3, 7]
γ_F^{-1}	Time from death until burial	days	1 - 3	[3, 23]
γ_R^{-1}	Duration of ETU bed occupancy after recovery	days	5 - 15	[9],*
δ	Overall mortality rate (fraction)	unitless	Estimated	Estimated
δ_2	Mortality rate (fraction) among those in second stage of illness	unitless	0.9 - 1	[7]
k	Fraction of the population at risk, symptomatic fraction, and reporting rate	unitless	0.001 - 1 [†]	See methods

Table 1: Model parameters, definitions, units, sources, ranges, and (if applicable) the default value used in the simulations for the stage structured model (Eq. (1)). *Personal communication with clinicians on the ground in Liberia. [†]This range was used for all simulations except when fitting Guinea in Figure 2, where a wider range from 0.00025 - 1 also yielded equally good fits to the data and was used.

case counts somewhat simpler to work with. To address the issue of artificially smaller confidence intervals, and to address the fact that the data are largely exponential (meaning there are inherent identifiability issues in fitting anyhow), we instead combine least squares optimization of only two parameters with LH sampling of all remaining parameters. This forces the model to sample across the full range of parameter values and model trajectories that are within the realistic biological ranges in Table 1 (all of which can generate qualitatively good fits that are consistent with the observed data once β_1 and δ are fitted). We then use these bounds rather than traditional confidence intervals for our forecasting and estimates. Essentially, this uses the biological ranges for the parameters to generate our ranges of estimates for the parameters and forecasts, rather than likelihood-based criteria which may suffer from issues of unidentifiability and lack of independence in the data.

The model initial conditions were determined as follows: $y_C(0)$ and $y_D(0)$ were both set equal to the initial values of the data set being fitted; $I_2(0)$ was approximated by examining the number of new deaths reported in the next two days after the first data point (as these would have been in I_2 as of $t = 0$), and then re-scaling this quantity from numbers of individuals to fraction of the population using k and N ; $I_1(0)$ was approximated by evaluating the number of cases that had

	Parameter	LHS Overall Best Estimate	Range of LHS Estimates (Median)
All Countries	β_1	0.11	0.079 - 0.18 (0.12)
	δ	0.56	0.55 - 0.6 (0.57)
	\mathcal{R}_0	1.60	1.43 - 1.64 (1.53)
Guinea	β_1	0.16	0.078 - 0.18 (0.11)
	δ	0.65	0.64 - 0.72 (0.68)
	\mathcal{R}_0	1.79	1.47 - 1.79 (1.61)
Liberia	β_1	0.12	0.0725 - 0.17 (0.10)
	δ	0.63	0.63 - 0.72 (0.67)
	\mathcal{R}_0	1.81	1.34 - 2.75 (1.47)
Sierra Leone	β_1	0.12	0.085 - 0.17 (0.12)
	δ	0.38	0.36 - 0.38 (0.37)
	\mathcal{R}_0	1.32	1.19 - 1.37 (1.25)

Table 2: Estimated values for β_1 , δ , and \mathcal{R}_0 , using the stage structured model. All remaining parameters were either set to the default values, or LH sampled from the ranges in Table 1, with the overall best fit across all samples shown (middle), and the range and median of LH sample parameter estimates in the right column.

been reported in the past six days (as these would, on average, still be in I_1) and then re-scaling as for I_2 ; $F(0)$ was approximated by the re-scaled number of deaths reported within the previous two days; $R(0)$ was approximated roughly by taking the number of incident cases in the last 15 days, subtracting the number of dead in the last 15 days, and then re-scaling to fractions of the population; $E(0)$ was taken as twice the initial values for infectious individuals. $S(0)$ was then calculated as 1 minus the remaining model variable initial values. These initial conditions are quite rough (reflecting the uncertainty in the data as well), but we tested a wide range of initial conditions based on differing assumptions and even sampling within realistic ranges for the initial conditions, and found that the model fit well to the data (with similar residual sum of squares values) for all initial condition values we set.

3.3 Fitting and Forecasting Results

Table 2 shows the estimated values for β_1 , δ , and \mathcal{R}_0 for each of the data sets. All remaining parameters are sampled from the ranges in Table 1 using Latin Hypercube (LH) sampling, with the overall best fit across all LH samples, range of estimates, and median of of the LH sample estimates each shown. The remaining LH sampled parameters that resulted in the overall best fit in Table 2 were:

- All countries: $\alpha = 0.1$, $\beta_2/\beta_1 = 3.38$, $\beta_F/\beta_1 = 3.44$, $\delta_2 = 0.99$, $\gamma_F = 0.36$, $\gamma_2 = 0.53$, $\gamma_1 = 0.19$, $k = 0.0026$
- Guinea: $\alpha = 0.11$, $\beta_2/\beta_1 = 2.04$, $\beta_F/\beta_1 = 2.63$, $\delta_2 = 0.99$, $\gamma_F = 0.40$, $\gamma_2 = 0.92$, $\gamma_1 = 0.19$, $k = 0.0006$

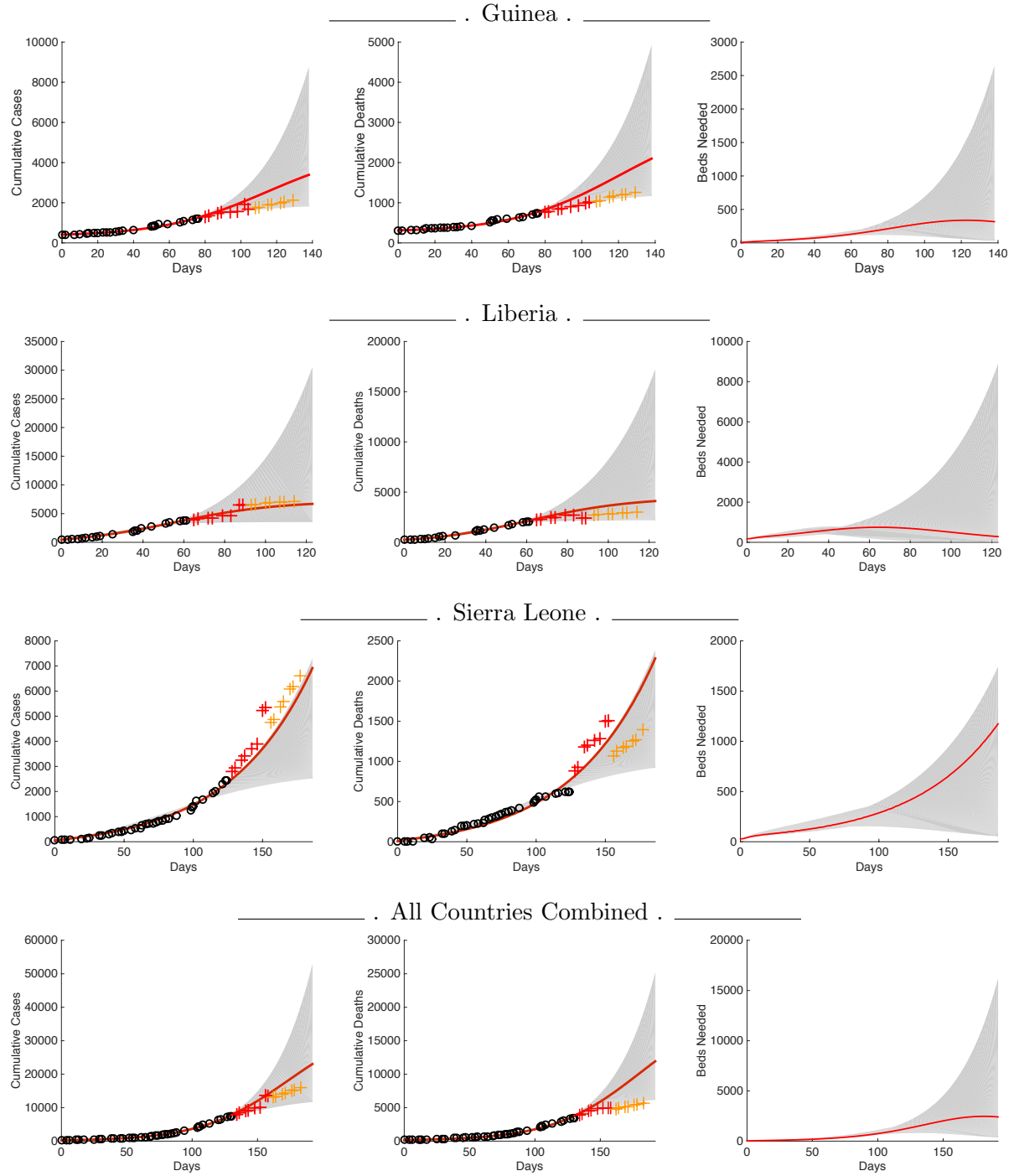


Figure 2: Simplified Model fit to total cumulative cases and deaths up through October 1, 2014. Grey region shows the full range of best-fit trajectories for the parameter ranges in Table 1. The model dynamics using overall best fit parameters across all LH-sampled values is shown in red. Data used for fitting is shown as circles, subsequent data not used for fitting shown as red +’s for October and orange +’s for November.

- Liberia: $\alpha = 0.11$, $\beta_2/\beta_1 = 4.90$, $\beta_F/\beta_1 = 3.84$, $\delta_2 = 0.93$, $\gamma_F = 0.35$, $\gamma_2 = 0.96$, $\gamma_1 = 0.20$, $k = 0.0024$
- Sierra Leone: $\alpha = 0.10$, $\beta_2/\beta_1 = 1.73$, $\beta_F/\beta_1 = 2.97$, $\delta_2 = 0.92$, $\gamma_F = 0.38$, $\gamma_2 = 0.73$, $\gamma_1 = 0.15$, $k = 0.68$

We note that since γ_R does not affect the model goodness-of-fit (since recovered individuals are assumed not to transmit the virus), we took γ_R to be the default value in Table 1 for the best-fit simulations.

Figure 2 shows the fits to data with projections of the numbers of cases, deaths, and beds needed through the December 1, 2014. The number of beds needed was calculated as the total infected and recently recovered, $kN(I_1 + I_2 + R)$ (though we note that k includes the reporting rate). The model predictions show a wide range of potential trajectories, consistent with the uncertainty associated with fitting to epidemic data in the exponential growth phase. The parameter k was particularly sensitive, and responsible for the majority of the breadth in trajectories for cumulative cases and deaths (for example, the fit using the default parameters could in general be adjusted to cover the full shaded range of cases and deaths just by adjusting k and re-fitting β_1 and δ). For comparison purposes, we also show the reported data for cases and deaths from October 1 - 31 (red +’s), and from November 1 - 26 (orange +’s), although we emphasize that our model projections do *not* account for changes in reporting rate or effects of interventions, both of which are known to have been significant during October and November [2, 13]. In particular, there are several sudden increases and decreases in reported cumulative cases reported which are due to changes in reporting [2], which the model does not capture as we use a constant reporting rate (in particular, the model cannot capture decreases in cumulative cases). Nonetheless, the forecast from the LH sampled best-fit trajectory (red line) was generally close to the reported data, and captured the correct qualitative behavior in all cases (i.e. continued exponential growth vs. slowing down of the epidemic). The forecasts matched the first month of data (red +’s) quite closely, with wider deviations in comparing with the second month of data (orange +’s).

We note that the sum of square residuals was often quite close for many of the fitted parameters in the range, so that a wide range of parameter values were able to yield similarly good fits (indicating practical unidentifiability of the parameters, as might be expected when fitting to exponential growth data). Supp. Figure 10 shows histograms of the residual sum of squares values for all fits. The trajectories with the lowest squared residuals did tend to cluster near the best fit line in Figure 2, as shown in Supp. Figure 11 (which shows the best 10% of all LH-sampled fits). Even among these best 10% of fits, several of the LH-sampled parameter estimates still show a fairly broad range, highlighting that the parameter uncertainty/unidentifiability persists even if the goodness of fit scores are restricted more tightly. In particular, the transmission parameters by stage were often able to generate very similar fits and forecasts for a wide range of parameter values. This suggests these parameters may form an identifiable combination [44, 45], wherein decreases in transmission levels in one stage can be compensated for by increasing transmission in another stage, so that the individual transmission parameters cannot be estimated (are unidentifiable), but the overall transmission level is estimable. This compensation manifests in parameter space as a plane of best fit parameter estimates, shown in Supp Fig. 14.

3.4 Transmission & Interventions by Stage

Next, we examined the contributions of each stage to transmission. The model \mathcal{R}_0 breaks up into contributions by each of the three stages (with each term in Eq. (2) corresponding to I_1 , I_2 , and F), which makes a natural way to evaluate the relative contributions of each transmission stage to

	\mathcal{R}_0	\mathcal{R}_1	\mathcal{R}_2	\mathcal{R}_F
All countries	1.6 (1.43 - 1.64)	0.58 (0.45 - 1.0) 36% (30% - 69%)	0.41 (0.10 - 0.61) 26% (7% - 40%)	0.61 (0.22 - 0.86) 38% (14% - 56%)
Guinea	1.79 (1.47 - 1.79)	0.86 (0.41 - 1.0) 48% (26% - 63%)	0.23 (0.12 - 0.70) 13% (7% - 43%)	0.69 (0.26 - 0.97) 39% (16% - 57%)
Liberia	1.81 (1.34 - 2.75)	0.60 (0.38 - 0.99) 33% (28% - 62%)	0.41 (0.11 - 0.70) 22% (8% - 47%)	0.81 (0.24 - 1.1) 45% (16% - 57%)
Sierra Leone	1.32 (1.19 - 1.37)	0.84 (0.49 - 0.96) 64% (39% - 75%)	0.12 (0.065 - 0.41) 9% (5% - 34%)	0.36 (0.15 - 0.55) 27% (12% - 44%)

Table 3: Overall best estimates and ranges for \mathcal{R}_0 , and the contribution to \mathcal{R}_0 by I_1 , I_2 , and F (denoted \mathcal{R}_1 , \mathcal{R}_2 , and \mathcal{R}_F respectively), as both magnitude and percentage of overall \mathcal{R}_0 .

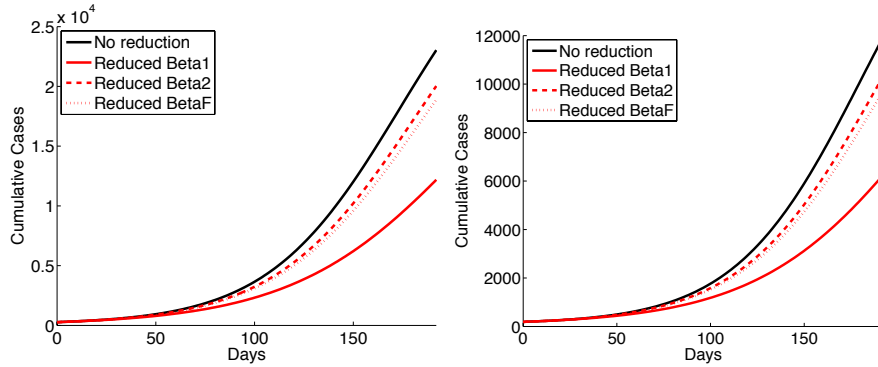


Figure 3: Simulated cases and deaths for all countries combined, assuming the overall best LHS parameter estimates (black line), and with 10% reductions in β_1 (red line), β_2 (red dashed line), or β_F (red dotted line).

the epidemic. Each term can be interpreted as the average number of secondary cases generated by an infectious individual while in a particular stage of transmission. We denote each of these terms as \mathcal{R}_1 , \mathcal{R}_2 , and \mathcal{R}_F respectively. Table 3 shows the contributions to \mathcal{R}_0 by each stage. In all cases all three transmission stages contributed to \mathcal{R}_0 , with I_1 and F tending to make the largest contributions to \mathcal{R}_0 . We note that the estimated ranges of contribution by each stage are quite wide, likely due to the unidentifiability issues for the transmission parameters by stage as noted above.

Next, we evaluated the dynamic effects of potential reductions in transmission by stage, using the all countries combined simulations as an example. We simulated the total cases and deaths using the overall best fit parameters from Table 2, supposing a 10% reduction in each of the transmission parameters (β_1 , β_2 , β_F), with results shown in Figure 3. The reduction in β_1 was most effective, followed by β_F and then β_2 .

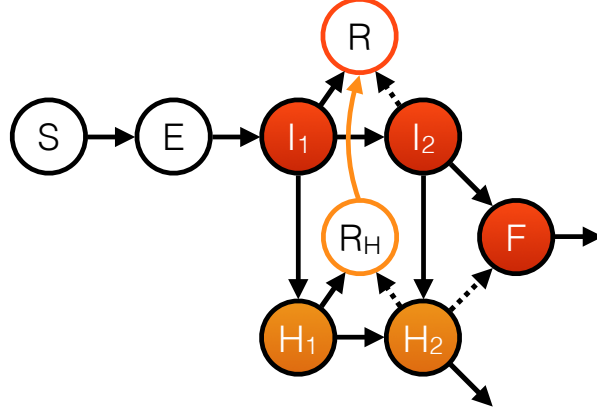


Figure 4: Expanded Ebola model, with both multi-stage infection and hospitalization. ETU/hospital compartments are shown in orange, non-ETU compartments in red. Transmissible compartments are shaded. R_H represents the recently recovered (who are still occupying an ETU bed).

4 Hospital Intervention Simulations

4.1 Expanded Model Structure and Parameter Estimates

In order to evaluate the effect of ETU dynamics and potential interventions, we next consider an expanded model which explicitly distinguishes between hospitalized and non-hospitalized populations by stage of infection, shown in Figure 4. The corresponding equations are:

$$\begin{aligned}
\frac{dS}{dt} &= -(\beta_1(I_1 + \beta_H H_1) + \beta_2(I_2 + \beta_H H_2) + \beta_F F)S \\
\frac{dE}{dt} &= (\beta_1(I_1 + \beta_H H_1) + \beta_2(I_2 + \beta_H H_2) + \beta_F F)S - \alpha E \\
\frac{dI_1}{dt} &= \alpha E - \gamma_1 I_1 - h_1 f(H_{max}) I_1 \\
\frac{dI_2}{dt} &= \delta_1 \gamma_1 I_1 - \gamma_2 I_2 - h_2 f(H_{max}) I_2 \\
\frac{dH_1}{dt} &= h_1 f(H_{max}) I_1 - \gamma_1 H_1 \\
\frac{dH_2}{dt} &= h_2 f(H_{max}) I_2 + \delta_{1H} \gamma_1 H_1 - \gamma_2 H_2 \\
\frac{dF}{dt} &= \delta_2 \gamma_2 I_2 + \delta_{2H} \delta_{2B} \gamma_2 H_2 - \gamma_F F \\
\frac{dR}{dt} &= (1 - \delta_1) \gamma_1 I_1 + (1 - \delta_2) \gamma_2 I_2 + \gamma_R R_H \\
\frac{dR_H}{dt} &= (1 - \delta_{1H}) \gamma_1 H_1 + (1 - \delta_{2H}) \gamma_2 H_2 - \gamma_R R_H
\end{aligned} \tag{4}$$

where S , E , and F are as in (1), but the infected and recovered classes have now been split into ETU/hospitalized (H_1 , H_2 , and R_H) and community compartments (I_1 , I_2 , and R). For the hospitalized recovered (R_H), we consider only the recently recovered who would still occupy a bed in an ETU/hospital (after which point they join the recovered in the community). The parameter β_H represents the ratio of transmission for hospitalized vs. non-hospitalized patients, and the fractions

of ETU patients who progress from the first stage, die during the second stage, and have transmissible burials are given by δ_{1H} , δ_{2H} , and δ_{2B} respectively. The parameters h_1 and h_2 represent the hospitalization rates for I_1 and I_2 respectively. The remaining parameters are as in (1).

ETU Capacity. To explicitly account for the time-varying capacity of the ETUs we use $f(H_{max})$, which we define to be a smoothed switch (Heaviside) function that is zero when the total number of occupied beds ($H_1 + H_2 + R_H$) is greater than or equal to the maximum ETU beds, H_{max} , and one otherwise. Thus, the ETUs fill to capacity at rates h_1 and h_2 , at which point they can no longer admit patients. To estimate maximum capacity H_{max} for ETUs over time, we used WHO reports of the total beds available [2], and linearly interpolated between points. We roughly approximated the initial number of beds (starting May 24, 2014) as 25% of the first reported number of beds (853 beds reported September 21, 2014).

Measurement Equations. To connect the model with data, we supposed that all hospital cases are reported, but that the community cases are measured with a reporting rate of 1/2.5 (based on CDC reporting rate estimates [9], though we also tested a range of reporting rates from 1/1.5 to 1/10 with similar results). As our previous form of k using the simplified model combined the reporting rate with several other potential correction factors, we thus take the new value for k to be 2.5 times the best estimate from the simplified model using all countries combined (Table 2). Similarly to the simplified model, the new measurement equations y_C and y_D are then given by summing up the cumulative hospitalized cases and deaths, plus community cases and deaths divided by 2.5.

The expanded model, while more realistic, also includes significantly more parameters and initial conditions than the simplified model (Figure 1). For simplicity we illustrate the effects of different interventions by only fitting β_1 with the rest of the parameters fixed to values determined from the literature, WHO, and values fitted using the simplified model in previous sections. The full set of parameters for the expanded models are given in Table 4. Most parameters are as in Table 1, but we updated β_2 , β_F , and k based on the overall best fit values using the stage structured model. The parameter δ_{2B} (the fraction of deaths in ETUs with the potential for funeral transmission) was set to be small, as ETUs do their best to ensure safe burial of patients who die. However, to account for limited resources and burial teams, and the possibility that some bodies may still be buried with the potential for transmission (e.g. if families remove the body), we set δ_{2B} to be nonzero (0.1). The parameter h_2 , the hospitalization rate in the second stage of illness, was set to be 50% faster than γ_2 , supposing that hospitalization once more severe symptoms begin will be relatively rapid. We estimated β_1 using the same least squares approach as for the simple model, with the rest of the parameters as given in Table 4. The resulting fits to data and dynamics of occupied and needed beds are given in Figure 5.

4.2 Intervention Strategies

Using the expanded model, we examined three types of interventions: 1) increasing ETU beds and capacity (H_{max}), 2) increasing the staff and supplies at the ETU's (and thereby reducing hospital transmission and deaths), and 3) increased case-finding and safe burials, resulting in increased hospitalization rates and reductions in funeral transmission. To evaluate the potential effects of these three interventions on the current outbreak trajectory, we began the interventions on Oct 1, 2014, coinciding with the beginning of the UN Mission for Ebola Emergency Response (UNMEER) [13], as well as ongoing increases in a wide range of other intervention efforts [11, 12, 46]. We modeled each of these intervention strategies at baseline, moderate, or high levels, as follows:

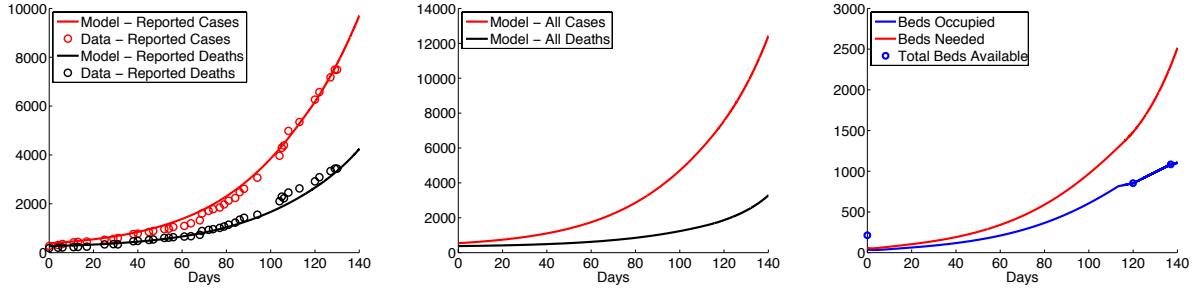


Figure 5: From left to right, expanded Ebola model fitted to cumulative reported incidence (red) and reported deaths (black) for all countries combined from May 24, 2014 to October 1, 2014; model estimates for total cumulative cases and cumulative deaths; dynamics of beds daily occupied (blue) and needed (red).

- **Treatment & Isolation Capacity** - WHO reports suggest that an estimated 6319 ETU beds were needed as of December [2]. To model this increase in capacity, we considered three ETU capacity intervention levels:

- Baseline: stayed at the levels available on October 1, 2014 (~ 1084 beds),
- Moderate: increased linearly to full capacity by January 1, 2014,
- High: increased linearly to full capacity by December 1.

We also note the model simulation of capacity represents not just beds, but also the number of people that can be isolated, which has increased to an estimated 70% of all cases as of December [2]. For example, depending on the severity of symptoms, not all cases may need ETU beds in order to be isolated (e.g. in the early stages of infection). We note that this increase in capacity also supposes a proportional increase in staff and supplies as well as beds (as otherwise the additional beds would not be usable and/or we would expect increases in hospital transmission and deaths due to lack of support and supplies).

- **Additional Staff and Supplies (S&S)** - We supposed that additional increases in staff and supplies (such as PPE, medical equipment, drugs) would reduce transmission and death rates in the ETUs, as well as reducing the amount of time recovered patients need to occupy a bed (due to faster recovery times and more rapid Ebola testing before being released). For the reduction in death rate, we supposed that this would be more pronounced for individuals hospitalized earlier (as has been seen in clinics for several Ebola outbreaks including the current one [7?]). We considered the following intervention levels:

- Baseline: the existing, fitted parameters from data up through Oct. 1, 2014,
- Moderate: 50% reduction in the ETU transmission rate (β_H), fraction of H_1 that progress to second stage of illness (δ_{1H}), and bed occupancy time (γ_R^{-1}),
- High: 75% reduction in the above parameters.

- **Case-finding & Safe Burials (C&S)** - Lastly, we considered the potential for increased case-finding and reductions in funeral transmission (e.g. as community health workers and burial teams are mobilized). We supposed that increased case-finding would increase the rate of hospitalization, particularly in the early stages of illness. We considered the following intervention levels:

- Baseline: no change after October 1, 2014,

- Moderate: increased the early stage hospitalization rate (h_1) by a factor of 2.5, and reduction of hospital contribution to unsafe burials (δ_{2B}) to zero (noting that the default level was fairly low to begin with),
- High: increased early-stage hospitalization by a factor of 5, reduction of hospital contribution to unsafe burials to zero, and reduction in the number of transmissible community burials by 25%.

For both S&S and C&S interventions beyond baseline, we supposed that the parameters changed linearly from baseline over Oct 1 - Dec 1.

For comparison purposes, we also examined how these compare to a hypothetical minimal level of intervention, in which we supposed recent increases in capacity had not occurred. In this scenario, we supposed a maximum capacity of 400 beds (roughly half the capacity reported as of September 21) and the same parameters as in Table 4 (equivalent to the baseline levels of intervention for S&S and C&S).

Lastly, to evaluate the effects of timing of interventions, we also simulated beginning interventions at a range of start dates from the beginning of the epidemic to December 1. We supposed moderate level interventions for S&S and C&S and either constant capacity of 4500 beds beginning at the start date, or linear increase in bed capacity from 200 beds at the start date up to 4500 beds as of December 1.

4.3 Intervention Simulation Results

The expanded model fit to the WHO data on reported cumulative cases and deaths is shown in Figure 5, together with the resulting simulations for total cumulative cases and deaths (in addition to those reported), as well as the daily number of beds needed, available, and occupied. The difference between reported and actual total cases decreases as time goes on and ETU capacity increases, and we see that although ETU capacity increased, it was not fully able to keep up with demand. The estimated value of β_1 for the expanded model (Table 4) was higher than that of any of the simplified stage-structured model estimates (Table 2), consistent with the idea that the simplified model combined hospitalized and non-hospitalized populations (thus yielding transmission parameter estimates between the community and ETU transmission parameter estimates here).

Figure 6 illustrates the effects of each level of intervention, showing minimal, baseline, moderate, and high levels of interventions for all three intervention types (capacity, S&S, C&S). The fit to the data and forecasts are consistent with there having been increasing intervention efforts, potentially at even higher levels than those tested in these simulations (in the case of cumulative deaths). However, the decreases in cumulative cases seen in the data indicate that some of the slowdown in the epidemic seen in the data is likely due to changes in reporting. While the maximal number of beds occupied initially increased as intervention efforts increased, at the highest levels of intervention efforts, the maximal beds occupied decreased, because transmission interruptions were sufficiently large to reduce the number of beds needed.

Figure 7 shows the effects of different levels of intervention in S&S and C&S, assuming either a baseline, moderate, or high level of interventions in ETU capacity. Sufficient ETU capacity acted as a prerequisite for S&S and C&S interventions, so that these two interventions yielded only minimal changes in the total cases and deaths when the ETU capacity was low, but showed stronger effects once ETU capacity increased.

Figures 8 and 9 show how the timing of interventions affects the epidemic. In Figure 8, we simulated constant intervention efforts (moderate C&S, S&S, together with an ETU capacity of 4500 beds) starting at different dates, and tracked total cases and maximal numbers of beds

	Definition	Units	Estimate	Source
β_1	Transmission parameter for first stage of illness	people ⁻¹ days ⁻¹	0.24	Estimated
β_H	Ratio of infectiveness in hospital vs. community	unitless	0.1	[2, 31]
$\frac{\beta_2}{\beta_1}, \frac{\beta_F}{\beta_1}$	Ratio of infectiveness in first vs. subsequent stages of illness	unitless	3	Tables 1 & 2
α^{-1}	Average incubation period	days	9	[3, 5]
h_1	Hospitalization rate in first stage of illness	days ⁻¹	0.1667	[47, 48]*
h_2	Hospitalization rate in second stage of illness	days ⁻¹	0.75	See methods
H_{max}	Total ETU beds available	beds	time-varying	[2]
γ_1^{-1}	Length of first stage of illness	days	6	[3, 7]
γ_2^{-1}	Length of second stage of illness	days	2	[3, 7]
γ_F^{-1}	Time from death until burial	days	2	[3, 23]
γ_R^{-1}	Duration of ETU bed occupancy after recovery	days	10	[9], [†]
δ_1	Overall mortality rate (fraction) in the community	unitless	0.9	[35, 49, 50]
δ_2	Mortality rate (fraction) among those in second stage of illness in the community	unitless	0.95	[7]
δ_{1H}	Fraction of H_1 that progress to second stage rather than recovering	unitless	0.6	[49, 50]
δ_{2H}	Mortality rate (fraction) among those in second stage of illness in ETUs	unitless	0.8	[7]
δ_{2B}	Fraction of deaths in ETUs with potential burial transmission	unitless	0.1	See methods
k	Fraction of the population at risk, symptomatic fraction	unitless	0.0026	Table 2

Table 4: Model parameters, definitions, units, estimates, and sources for the hospitalization model. Parameters which are new or updated from the simple model are shaded. *Determined from the listed sources and supposing that most hospitalizations occur towards the end of the first stage of infection. [†]Personal communication with clinicians on the ground in Liberia.

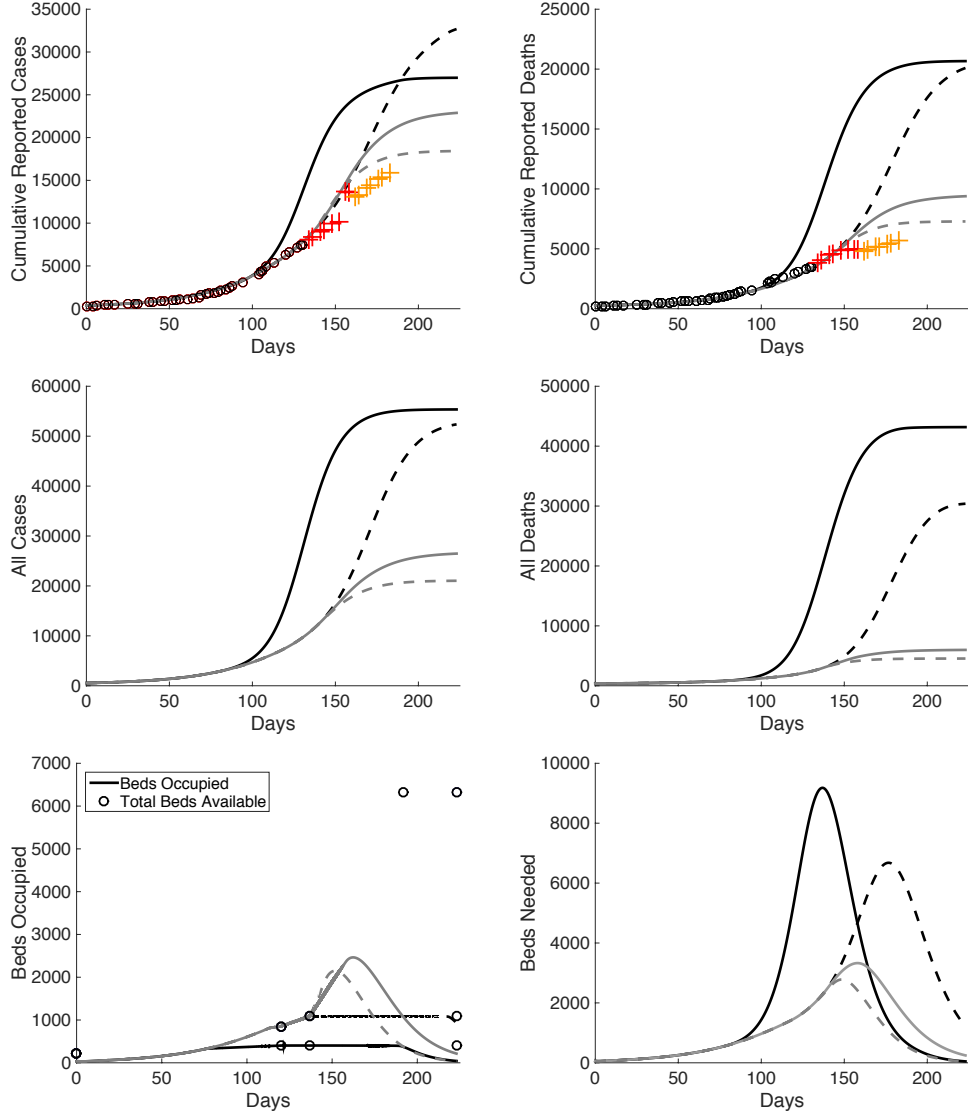


Figure 6: Model simulations up through January 1, 2014, showing minimal (black solid line), baseline (black dashed line), moderate (grey solid line), and high (grey dashed line) levels for all interventions. Top row: Data (o/+) and simulations (lines) of cumulative reported cases (left) and cumulative reported deaths (right), under each intervention scenario. Data used for fitting shown as black circles (o), forecasted data shown as red (October) and orange (November) plus signs (+). Middle row: Corresponding simulations of cumulative total cases (left) and cumulative total deaths (right). Bottom row: Simulations of beds occupied (left) and needed (right). Total ETU beds shown as blue circles.

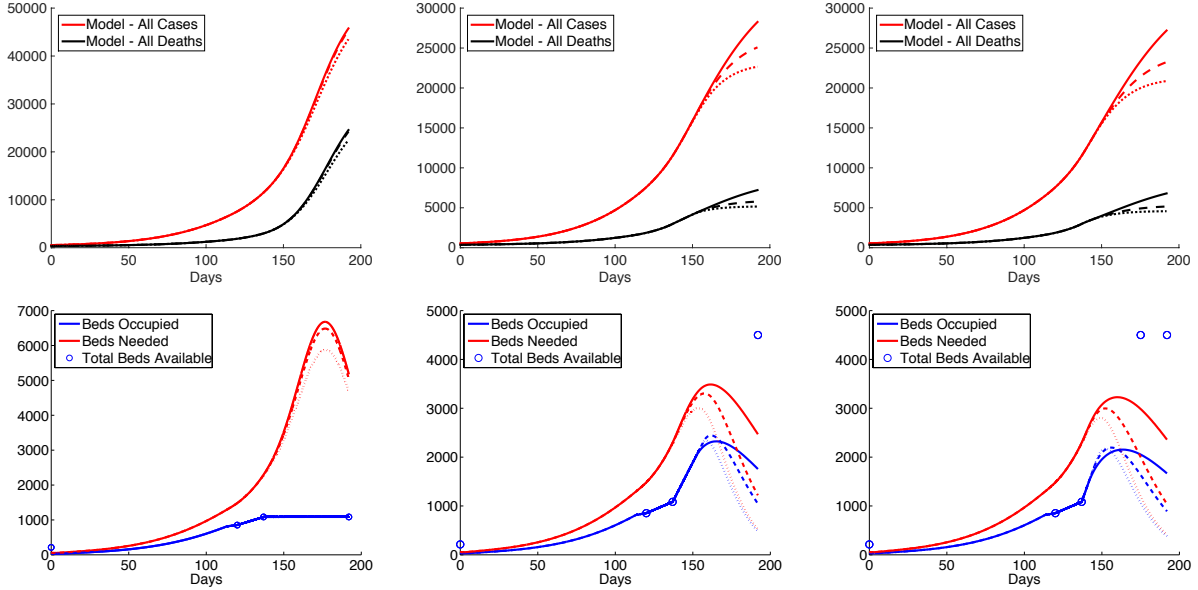


Figure 7: Model simulations using baseline (solid), moderate (dashed), or high (dotted) level interventions for both additional S&S and for C&S, supposing the underlying ETU capacity is at baseline (left), moderate increase (middle), and high increase (right). Adding additional supplies and staff and improving trust only begins to have a large effect when there is sufficient ETU capacity. Top row: Cumulative total cases (red) and deaths (black), including unreported/non-ETU cases, bottom row: daily beds available (blue circles), occupied (blue lines), and needed (red lines).

needed/occupied. We see that the total cases, total deaths, and maximum beds needed all increase as the intervention starts later, with a jump near 50 days where the ETU capacity first becomes insufficient to meet demand. The number of beds occupied plateaus around 100 days, where the interventions are late enough that a capacity of 4500 ETU beds is no longer close to sufficient to meet bed demand. Figure 9 shows a similar simulation set, but now supposing that each simulated intervention linearly increased from no effect at the start date to full effect by December 1 ($t = 192$), to represent a more realistic ramp-up in efforts.

5 Discussion

We developed a stage-structured model of EVD transmission dynamics, which captures, in a simplified form, the progression of illness in EVD (Figure 1). We fitted the model to data from the ongoing epidemic in West Africa using an LH sampling approach, and used the resulting distribution of fitted models to evaluate forecasting and parameter uncertainty, and examine the dynamics of surveillance, interventions, and contributions to the epidemic by stage of transmission.

The fits of the stage-structured model to the current outbreak data (Figure 2) generally agreed well with the data, and most parameters yielded similar ranges of estimates and similar overall best-fit values across each of the three countries (Table 2). The \mathcal{R}_0 estimates ranged from 1.19 to 2.75, with the highest estimates in Liberia, consistent with the higher initial growth rate and initially larger numbers of cases/deaths in the Liberia data. The overall best estimated death rates for each country (Table 2) also roughly correspond to the crude death rates reported based on dividing total deaths by total suspected cases [2].

However, we note that the inherent unidentifiability associated with fitting to exponential

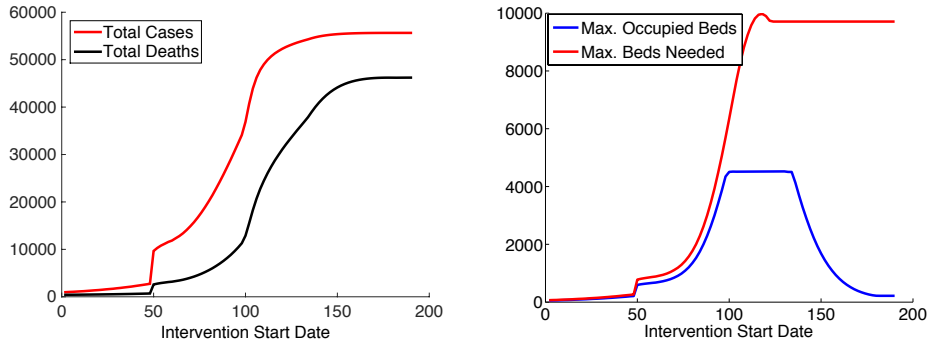


Figure 8: Simulations of total cases and deaths as of Dec 1, 2014 (left) and maximum daily levels of occupied and needed beds over the course of the epidemic (middle), as a function of the intervention start date, using constant moderate level interventions for capacity, supplies and staff, and trust. Right panel shows daily beds needed assuming no interventions.

growth data means that many of the sampled parameters fit the data similarly well. This resulted in a wide range of forecasted trajectories of cases and deaths in Figure 2 illustrating the large uncertainty and parameter unidentifiability associated with forecasting from exponential growth phase data, in which a range of parameter values can yield the same initial growth rate, but may differ as to when their resulting trajectories begin to slow from exponential growth. This also translates to similarly broad estimates for numbers of ETU beds needed. The uncertainty increases the further into the future we forecast, as do the errors between the model forecast and the reported data, illustrating the difficulty in generating long-term projections. Some of the error in forecasting may also be due to changing conditions on the ground, such as the known increases in interventions and changes in reporting [2, 13], which would not be captured in the model, as it was fitted using constant parameters and based only on the data up through October 1. For example, the data during the forecasting period showed several drops in cumulative cases, likely reflecting changes in reporting that would not be possible to capture in the current model.

These unidentifiability issues suggest the potential for identifiable combinations wherein changes in one parameter can be compensated for by adjusting another parameter. In particular, the transmission parameters by stage and the durations of the later stages tended to be able to generate similar fits for a wide range of values (Supp. Fig. 12 and 11), suggesting that these parameters may form identifiable combinations, e.g. so that increasing the transmission parameter of one stage can be compensated by decreasing that of another stage. This manifests as an approximate plane of best fit parameter estimates, shown in Supp Fig. 14. This issue has also been noted for infected and funeral transmission in [40] using the SEIRD model, wherein they also note that the unidentifiability issues are likely to persist more broadly in models fitted to exponential growth data, as is the case here.

Nonetheless, a key finding was that the overall best fit models were able to successfully forecast the reported data not used in fitting, particularly for Liberia and Sierra Leone. Recent commentary [51] has noted that many models were unable to forecast the decline in new cases seen in Liberia (although we note that the models referenced in [51] were not intended to account for how changes in reporting or interventions would affect the epidemic trajectory, as discussed further in [52]). However, our overall best-fit model projected the correct qualitative behavior in all cases, accurately forecasting a plateauing epidemic in Liberia and continued growth in Guinea and Sierra Leone. The best-fit model trajectories matched the data particularly closely for the first month of forecasted data (red +’s) in all cases. This suggests that even though the slow-down in the Liberia data

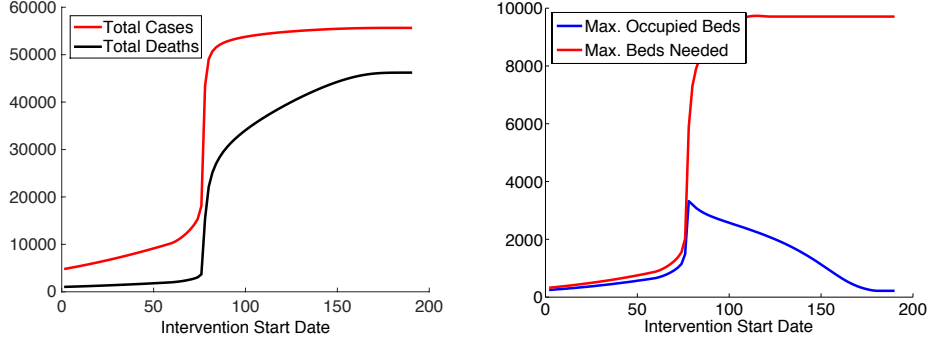


Figure 9: Simulations of total cases and deaths as of Dec. 1, 2014 (left) and maximum daily levels of occupied and needed beds over the course of the epidemic (right), as a function of the intervention start date, where we assumed a linear increase to the moderate level interventions for capacity, supplies and staff, and trust beginning on the start date and reaching full strength on Dec. 1, 2014.

may not be evident by eye as of October 1, the model was able to detect hints in the data of the upcoming change in dynamics which were reflected in the best-fit model.

These results illustrate that in spite of the large uncertainty, model forecasts can still provide estimates of the qualitative behavior of the epidemic, and even broad forecasts may be more useful than a lack of information. Forecasting efforts may be particularly useful for comparing alternative scenarios as to potential intervention effects (as discussed further below). Moreover, understanding the uncertainty inherent in these forecasts can itself be useful in evaluating the range of intervention efforts that may be needed based on current data, and could potentially help in guide additional data collection efforts to reduce this uncertainty [53]. Comparative modeling approaches could also be useful in this process [53], as different model structures and approaches may result in further uncertainty, or potentially provide some consensus across a range of different model assumptions.

Accurate forecasting depended heavily on including the correction factor k , the scaling correction used to account for wide range of factors, including underreporting, the size of the population at risk (e.g. due to contact patterns, etc.), asymptomatic cases, and potential errors in the initial conditions. The range of values sampled for k generated much of the breadth of the forecasted trajectories, with low values of k resulting in the bottom portion of the shaded region in Figure 2 and higher values corresponding to the top portion of the shaded region. As k is something of a ‘catch-all’ parameter, the biological/epidemiological meaning is not completely clear, but we hypothesize that part of the reason why the fits and forecasts are so sensitive to k is that k may also be an ad hoc way to represent the effects of changing conditions on the ground, shifts in behavior in the population, and ongoing intervention efforts. As interventions and changes in behavior reduce transmission, this may result in a lower effective fraction of the population at risk (decreasing k), so that the overall epidemic burns out earlier than it otherwise would due to the reduction in the likelihood of susceptible individuals becoming ill. A lower value of k thus results in a fitted model with a rapid increase matching the exponential growth in the data, followed by the epidemic beginning to turn over/burn out as the effective population at risk is smaller (perhaps due to removing individuals from the at-risk population by reductions in transmission).

Our best-estimates yield the much smaller values of k for Guinea, Liberia, and all countries combined than for Sierra Leone, which is consistent with the subsequent reports from October and November that indicate decreases in incidence in Liberia and Guinea with continued growth in Sierra Leone [2]. A related modeling study [10] recently showed that forecasts will tend to overestimate incidence if asymptomatic infections and their resulting immunity are not taken into account, which

illustrates another example of the phenomenon observed here. There are a wide range of factors which may alter the apparent population at risk, including asymptomatic infections, pre-existing immunity, reporting rate, social contact structures, and ongoing interventions. Our results show that accounting for these effects, even in the extremely simplified and agglomerated way used here, can make a significant difference the accuracy of the model forecasts—the model best fit without including k (i.e. with $k = 1$) is the top edge of the grey shaded regions in Figure 2, and overestimates the incidence in three of the four cases. By contrast, the best-fit model trajectories (red lines in Figure 2) consistently capture the qualitative (and for the first month quantitative) behavior actually observed in the data.

The basic reproduction number for this model breaks naturally into three pieces corresponding to the contributions from each stage (Eq. (2)). In an interesting contrast to the estimated transmission parameter values, when we evaluated the contribution of each stage of transmission to \mathcal{R}_0 in the West Africa epidemic, we found that while all three stages were significant contributors, second stage transmission tended to make a lower contribution to the overall \mathcal{R}_0 , for both individual countries and for all countries combined. The first stage, while less transmissible, lasts a longer period of time, and at each subsequent stage some fraction of people recover (and so don’t continue to transmit), lending the first stage a stronger impact on the overall \mathcal{R}_0 . The larger contribution in the first 5-7 days found here is similar to the estimates by [29] for the corresponding days of symptomatic disease. However, it is important to note that because of the unidentifiabilities in the transmission parameters, without additional biological knowledge or data, it is difficult to estimate precisely where in these ranges the contribution of each stage to \mathcal{R}_0 actually sits.

Nonetheless, in many of our simulations, even complete elimination of any single stage of transmission was not enough to reduce \mathcal{R}_0 below one, suggesting that interventions must target more than just the second stage to be fully effective (or indeed any other single stage), and highlighting the importance of earlier case-finding and reducing funeral transmission. In particular, interventions such as providing home health kits [54] may have a significant effect on early transmission and provide a useful complement to ETUs. Indeed, our simulations in the all countries combined case showed that reducing early stage transmission (β_1) by 10% was more effective at reducing the cumulative number of cases than reducing transmission from either of the later stages by the same fraction, consistent with the \mathcal{R}_0 results (Figure 3).

Next, we evaluated how changing ETU capacity affects both the outbreak dynamics and the intervention efforts. We developed an expanded model to include hospitalization dynamics (Figure 4), using reported ETU bed capacity [2] as forcing function for the maximum bed capacity, to dynamically adjust hospitalization rates. The model fit well to the data (Figure 5), and illustrates how reported cases grew closer to the underlying totals as ETU capacity increased.

We simulated three types of ETU-related interventions: increasing ETU capacity, increasing staff and supplies (S&S), and community relationship-building to improve case-finding/early hospitalization and safe burials (C&S). The model simulations and forecasts suggest a significant effect of ongoing intervention efforts, with potentially thousands of cases prevented by the continuing increases in ETU capacity, staff, supplies, and community-relationships (Figure 6). The effects of intervention efforts were more difficult to see in the reported cases, since increasing capacity also increases reporting of cases. This means that increasing interventions can have a seemingly paradoxical effect on reported cases, in which one may see reported cases which are quite similar for different intervention levels, even though the actual underlying total cases are very different (Figure 6). Indeed, in some cases this effect can even make it appear that there are more cases generated with intervention efforts than without, even though the dynamics of total cases reveal the opposite. Some of these issues can be seen in the data, with some jumps in reported cases in Liberia believed to be due to improved reporting [2].

As might be expected, increasing ETU capacity, S&S, and C&S together was the most effective approach, with the potential to reduce total cases to as low as around 20,000 (after correcting for under-reporting), using the intervention levels we tested. We found that ETU capacity is a key prerequisite for the effectiveness of interventions (Figure 7). Unless there are sufficient resources for individuals to practically be admitted to an ETU, the effectiveness of the S&S and C&S interventions was significantly hindered.

Timing of intervention efforts also plays a crucial role, with a switch-like increase in the total numbers of cases and deaths when intervention efforts start too late (Figure 8). Notably, we found that even if intervention efforts reach their full strength at the same date late in the epidemic, significant reductions in total cases and deaths can still be achieved by beginning the intervention efforts earlier, even if at a very low level (Figure 9). As stronger/earlier intervention efforts are applied, the total bed capacity needed initially increases (as there are more hospitalized cases), but with high enough intervention efforts can then decrease, as sufficient transmission is interrupted to reduce the need for ETUs (Figures 6, 8, and 9).

There are several limitations to this work. The model is fitted to cumulative cases rather than incident ones—while this is easier to work with, there are known issues with lack of independence between subsequent data points, which can lead to significant underestimates of parameter and forecasting uncertainty [42]. To address this, we use a LH sampling approach, which forces the parameters to traverse the range of biologically feasible values while using parameter estimation with a subset of parameters to generate model trajectories which are consistent with the data. This uses the biological ranges for the parameters to generate our forecasting ranges rather than traditional likelihood-based approaches. Additionally, the model does not account for factors such as non-ETU related changes in reporting, differences in reporting between cases and deaths, and spatial spread and mobility, all of which are likely to be changing with time. Changing conditions on the ground may make forecasting further than 1-2 months a difficult task (as illustrated in Figure 2), and further work to capture these time-varying parameters is warranted.

Another direction for future work is in examining the stage structure of the clinical course of EVD in more detail. This model includes a simplified representation of the natural history of EVD using two stages. However, some clinical descriptions of EVD break the clinical course into three stages, for example, as described in [35]: “a few days of non-specific fever, headache, and myalgia, followed by a gastrointestinal phase in which diarrhoea and vomiting, abdominal symptoms, and dehydration are prominent. In the second week, the patient may recover or deteriorate, with a third phase of illness including collapse, neurological manifestations, and bleeding, which is often fatal.” Our model likely includes part of this gastrointestinal phase in each of the two stages, and further work expanding the stage structure would be warranted. Further, the effects of the complex dynamics of the viral load and immune response results have recently begun to be explored in modeling efforts [29], and further work in this area would be particularly useful for uncovering clinical features that can be used to optimize treatment approaches.

5.1 Conclusions

In this paper, we developed a stage-structured model of Ebola which we used to fit the data, evaluate uncertainty in forecasting, and estimate \mathcal{R}_0 . The simplified model shows that uncertainty in predictions and parameter estimates is high, largely due to the inherent unidentifiability involved in fitting to exponential growth data, although the best-fit model does capture the correct qualitative behavior and forecasts the data well, particularly for the first month. This is partly because we account for a wide range of values for k , a simplified parameter roughly representing the reporting rate, fraction asymptomatic, population at risk, changing conditions on the ground, as well as other

factors. This highlights the importance of collecting data on these issues if accurate forecasting using models is to be accomplished.

We found that while the second and funeral stages of infection were more transmissible, second-stage transmission made the lowest contribution to \mathcal{R}_0 , as the longer duration of the first infection stage and the higher funeral transmission parameters give these two stages more weight. This suggests that reductions in funeral transmission and provision of home health kits (which would likely predominantly protect first-stage transmission) may provide a useful complement to ETU-based interventions.

We also expanded the model to evaluate ETU dynamics. Interventions can have a large effect on the outbreak, and our model suggests that we are already seeing some effect of them in the current data. ETU capacity and timing of interventions are of key importance in reducing the total numbers of cases and deaths, and allow the other interventions to reach their greatest effectiveness. The largest reduction in cases and deaths is gained by including all intervention types tested—increased capacity, additional staff and supplies, increased case-finding/early hospitalization, and promotion of safe burials. This provides a quantitative illustration of a recent quote from Paul Farmer, founder of Partners in Health, who said that halting the spread of Ebola will require a combination of "staff, stuff, space, and systems" [55]. Our model shows that while basic ETU capacity can help blunt the spread of the epidemic, the greatest reductions in cases come with a combination strategy that slows multiple transmission routes simultaneously.

6 Acknowledgements

This work was supported by the National Institute of General Medical Sciences of the National Institutes of Health under Award Number U01GM110712 (supporting JNSE, MCE, RM, and EVW), and Award Number U54GM111274 (supporting MCE), as part of the Models of Infectious Disease Agent Study (MIDAS) Network. The content is solely the responsibility of the authors and does not necessarily represent the official views of the National Institutes of Health.

References

- [1] WHO Ebola Response Team. Ebola virus disease in west africa the first 9 months of the epidemic and forward projections. New England Journal of Medicine, 371(16):1481–1495, 2014. PMID: 25244186.
- [2] World Health Organization. Ebola response roadmap - Situation report, <http://www.who.int/csr/disease/ebola/situation-reports/en/>, 2014.
- [3] World Health Organization. Ebola Virus Disease Fact Sheet, updated September 2014. <http://www.who.int/mediacentre/factsheets/fs103/en/>.
- [4] K.A. Alexander, C.E. Sanderson, B.L. Lewis M. Marathe, C.M. Rivers, J. Shaman, J.M. Drake, E. Lofgren, V.M. Dato, M.C. Eisenberg, and S. Eubank. What factors might have led to the emergence of ebola in west africa? PLOS Neglected Tropical Diseases, In press, 2014.
- [5] US Centers for Disease Control and Prevention. Ebola (Ebola Virus Disease), <http://www.cdc.gov/vhf/ebola/>, 2014.

- [6] Paolo Francesconi, Zabulon Yoti, Silvia Deelich, Paul Awil Onek, Massimo Fabiani, Joseph Olango, Roberta Andraghetti, Pierre E. Rollin, Cyprian Opira, Donato Greco, and Stefania Salmaso. Ebola Hemorrhagic Fever Transmission and Risk Factors of Contacts, Uganda, 2003.
- [7] Roger Ndambi, Philippe Akamituna, Marie-Jo Bonnet, Anicet Mazaya Tukadila, Jean-Jacques Muyembe-Tamfum, and Robert Colebunders. Epidemiologic and Clinical Aspects of the Ebola Virus Epidemic in Mosango, Democratic Republic of the Congo, 1995. The Journal of Infectious Diseases, 179:S8 – 10, 1999.
- [8] US Centers for Disease Control and Prevention. Ebola Virus Disease Information for Clinicians in U.S. Healthcare Settings, <http://www.cdc.gov/vhf/ebola/hcp/clinician-information-us-healthcare-settings.html> (accessed dec 2014), 2014.
- [9] Martin I. Meltzer, Charisma Y. Atkins, Scott Santibanez, Barbara Knust, Brett W. Petersen, Elizabeth D. Ervin, Stuart T. Nichol, Inger K. Damon, and Michael L. Washington. Estimating the Future Number of Cases in the Ebola Epidemic — Liberia and Sierra Leone, 2014-2015. MMWR Surveill Summ, 63:1–14, 2014.
- [10] S. E. Bellan, J. R. Pulliam, J. Dushoff, and L.A. Meyers. Ebola control: effect of asymptomatic infection and acquired immunity. The Lancet, 384:1499–1500, 2014.
- [11] Médecins Sans Frontières. Ebola crisis update - 16th October 2014, <http://www.msf.org/article/ebola-crisis-update-16th-october-2014>, October 16, 2014.
- [12] The White House Office of the Press Secretary. FACT SHEET: U.S. Response to the Ebola Epidemic in West Africa, <http://www.whitehouse.gov/the-press-office/2014/09/16/fact-sheet-us-response-ebola-epidemic-west-africa>, September 16, 2014.
- [13] UN Mission for Ebola Emergency Response (UNMEER), <http://www.un.org/ebolaresponse/mission.shtml>, October 1, 2014.
- [14] Stanford Medicine News Center. Rebuilding trust key to fighting Ebola in Africa, <http://med.stanford.edu/news/all-news/2014/09/building-trust-and-shattered-health-systems-key-to-fighting-ebol.html>, September 24, 2014.
- [15] Jacque Wilson, CNN. Borders closing over Ebola fears, <http://www.cnn.com/2014/08/22/health/ebola-outbreak/>, August 22, 2014.
- [16] BBC. Ebola outbreak: Sierra Leone lockdown declared ‘success’, <http://www.bbc.com/news/world-africa-29305591> , September 22, 2014.
- [17] Alexandra Sifferlin, Time Magazine. Equipping homes to treat Ebola patients, <http://time.com/3481394/equipping-homes-to-treat-ebola-patients/> , Oct. 9, 2014.
- [18] Médecins Sans Frontières. Ebola: Massive Distribution of Home Disinfection Kits Underway in Monrovia, <http://www.doctorswithoutborders.org/news-stories/field-news/ebola-massive-distribution-home-disinfection-kits-underway-monrovia>, October 02, 2014.
- [19] World Health Organization. Experimental Ebola vaccines, <http://www.who.int/mediacentre/news/ebola/01-october-2014/en/index1.html>, accessed December 9, 2014.

- [20] H Nishiura and G Chowell. Early transmission dynamics of ebola virus disease (evd), west africa, march to august 2014. Euro Surveill, 19(36):20894, 2014.
- [21] Gerardo Chowell and Hiroshi Nishiura. Transmission dynamics and control of ebola virus disease (evd): a review. BMC medicine, 12(1):196, 2014.
- [22] Marcelo FC Gomes, Ana Pastore y Piontti, Luca Rossi, Dennis Chao, Ira Longini, M Elizabeth Halloran, and Alessandro Vespignani. Assessing the international spreading risk associated with the 2014 west african ebola outbreak. PLOS Currents Outbreaks, 2014.
- [23] Caitlin M Rivers, Eric T Lofgren, Madhav Marathe, Stephen Eubank, and Bryan L Lewis. Modeling the impact of interventions on an epidemic of ebola in sierra leone and liberia. PLOS Currents Outbreaks, Oct 16, Edition 1, 2014.
- [24] Cameron Browne, Xi Huo, Pierre Magal, Moussa Seydi, Ousmanne Seydi, and Glenn Webb. A model of the 2014 ebola epidemic in west africa with contact tracing. arXiv preprint arXiv:1410.3817, 2014.
- [25] David Fisman, Edwin Khoo, and Ashleigh Tuite. Early epidemic dynamics of the west african 2014 ebola outbreak: estimates derived with a simple two-parameter model. Plos Currents Outbreaks, 2014.
- [26] Gerardo Chowell, Cécile Viboud, James M Hyman, and Lone Simonsen. The western africa ebola virus disease epidemic exhibits both global exponential and local polynomial growth rates. arXiv preprint arXiv:1411.7364, 2014.
- [27] Abhishek Pandey, Katherine E Atkins, Jan Medlock, Natasha Wenzel, Jeffrey P Townsend, James E Childs, Tolbert G Nyenswah, Martial L Ndeffo-Mbah, and Alison P Galvani. Strategies for containing ebola in west africa. Science, 346(6212):991–995, 2014.
- [28] Maria A Kiskowski. A three-scale network model for the early growth dynamics of 2014 west africa ebola epidemic.
- [29] Dan Yamin, Shai Gertler, Martial L Ndeffo-Mbah, Laura A Skrip, Mosoka Fallah, Tolbert G Nyenswah, Frederick L Altice, and Alison P Galvani. Effect of ebola progression on transmission and control in liberia. Annals of internal medicine, 2014.
- [30] Gerardo Chowell, Nick W Hengartner, Carlos Castillo-Chavez, Paul W Fenimore, and JM Hyman. The basic reproductive number of ebola and the effects of public health measures: the cases of congo and uganda. Journal of Theoretical Biology, 229(1):119–126, 2004.
- [31] J Legrand, RF Grais, PY Boelle, AJ Valleron, and A Flahault. Understanding the dynamics of ebola epidemics. Epidemiology and infection, 135(04):610–621, 2007.
- [32] Pheny E Lekone and Bärbel F Finkenstädt. Statistical inference in a stochastic epidemic seir model with control intervention: Ebola as a case study. Biometrics, 62(4):1170–1177, 2006.
- [33] Joseph A Lewnard, Martial L Ndeffo Mbah, Jorge A Alfaro-Murillo, Frederick L Altice, Luke Bawo, Tolbert G Nyenswah, and Alison P Galvani. Dynamics and control of ebola virus transmission in montserrado, liberia: a mathematical modelling analysis. The Lancet Infectious Diseases, 2014.

- [34] World Health Organization. Ebola response roadmap - Situation report, October 29, 2014, http://apps.who.int/iris/bitstream/10665/137376/1/roadmapsitre_29Oct2014_eng.pdf?ua=1, 2014.
- [35] Nicholas J Beeching, Manuel Fenech, and Catherine F Houlihan. Ebola virus disease. *BMJ*, 349:g7348, 2014.
- [36] MARGARETHA Isaacson, P Sureau, G Courteille, and SR Pattyn. Clinical aspects of ebola virus disease at the ngaliema hospital, kinshasa, zaire, 1976. *Ebola virus haemorrhagic fever*, pages 15–20, 1978.
- [37] Odo Diekmann, JAP Heesterbeek, and Johan AJ Metz. On the definition and the computation of the basic reproduction ratio r_0 in models for infectious diseases in heterogeneous populations. *Journal of mathematical biology*, 28(4):365–382, 1990.
- [38] Pauline Van den Driessche and James Watmough. Reproduction numbers and sub-threshold endemic equilibria for compartmental models of disease transmission. *Mathematical biosciences*, 180(1):29–48, 2002.
- [39] The World Bank Group. Estimates of total populations for Liberia, Guinea, and Sierra Leone, <http://data.worldbank.org/indicator/SP.POP.TOTL>, 2014.
- [40] Joshua S Weitz and Jonathan Dushoff. Post-death transmission of ebola: Challenges for inference and opportunities for control. *arXiv preprint arXiv:1411.3435*, 2014.
- [41] The MathWorks, Inc., Natick, Massachusetts, United States. Matlab and statistics toolbox release 2014b.
- [42] Aaron A King, Matthieu Domenech de Cellès, Felicia MG Magpantay, and Pejman Rohani. Avoidable errors in the modeling of outbreaks of emerging pathogens, with special reference to ebola. *arXiv preprint arXiv:1412.0968*, 2014.
- [43] Scott F Dowell, Rose Mukunu, Thomas G Ksiazek, Ali S Khan, Pierre E Rollin, and CJ Peters. Transmission of ebola hemorrhagic fever: a study of risk factors in family members, kikwit, democratic republic of the congo, 1995. *Journal of Infectious Diseases*, 179(Supplement 1):S87–S91, 1999.
- [44] Marisa C Eisenberg and Michael AL Hayashi. Determining identifiable parameter combinations using subset profiling. *Mathematical biosciences*, 256:116–126, 2014.
- [45] Elliot M Landaw, Benjamin Chao-Min Chen, and Joseph J Distefano III. An algorithm for the identifiable parameter combinations of the general mammillary compartmental model. *Mathematical biosciences*, 72(2):199–212, 1984.
- [46] DoD News, Defense Media Activity. Army General Takes Command of Ebola Response Operation, <http://www.defense.gov/news/newsarticle.aspx?id=123496>, Oct. 26, 2014.
- [47] Daniel S Chertow, Christian Kleine, Jeffrey K Edwards, Roberto Scaini, Ruggero Giuliani, and Armand Sprecher. Ebola virus disease in west africa: clinical manifestations and management. *New England Journal of Medicine*, 371(22):2054–2057, 2014.

- [48] Alexander K Rowe, Jeanne Bertolli, Ali S Khan, Rose Mukunu, JJ Muyembe-Tamfum, David Bressler, AJ Williams, CJ Peters, Luis Rodriguez, Heinz Feldmann, et al. Clinical, virologic, and immunologic follow-up of convalescent ebola hemorrhagic fever patients and their household contacts, kikwit, democratic republic of the congo. Journal of Infectious Diseases, 179(Supplement 1):S28–S35, 1999.
- [49] Dennis Thompson, U.S. News. There’s No Ebola Cure, But Early Intensive Treatment Boosts Survival, <http://health.usnews.com/health-news/articles/2014/07/31/theres-no-ebola-cure-but-early-intensive-treatment-boosts-survival>, July 31, 2014.
- [50] Lenny Bernstein, The Washington Post. As Ebola cases accelerate, Liberia’s sick must fend for themselves, http://www.washingtonpost.com/world/africa/as-ebola-cases-accelerate-liberias-sick-must-fend-for-themselves/2014/09/13/6ee71468-3b61-11e4-9c9f-ebb47272e40e_story.html, September 13, 2014.
- [51] Declan Butler. Models overestimate ebola cases. Nature, 515(18), 2014.
- [52] Caitlin Rivers. Ebola: models do more than forecast. Nature, 515(492), 2014.
- [53] Eric T Lofgren, M Elizabeth Halloran, Caitlin M Rivers, John M Drake, Travis C Porco, Bryan Lewis, Wan Yang, Alessandro Vespignani, Jeffrey Shaman, Joseph NS Eisenberg, et al. Opinion: Mathematical models: A key tool for outbreak response. Proceedings of the National Academy of Sciences, 111(51):18095–18096, 2014.
- [54] Alexandra Sifferlin, Time Magazine. This Is How Ebola Patients Are Equipping Their Homes, <http://time.com/3481394/equipping-homes-to-treat-ebola-patients/>, Oct. 9, 2014.
- [55] P. Farmer and J. Mukherjee. Ebola: Countries need ‘staff, stuff, and systems’, <http://www.pih.org/blog/for-ebola-countries-need-tools-to-treat-patients-in-their-communities>.

7 Supplementary Information

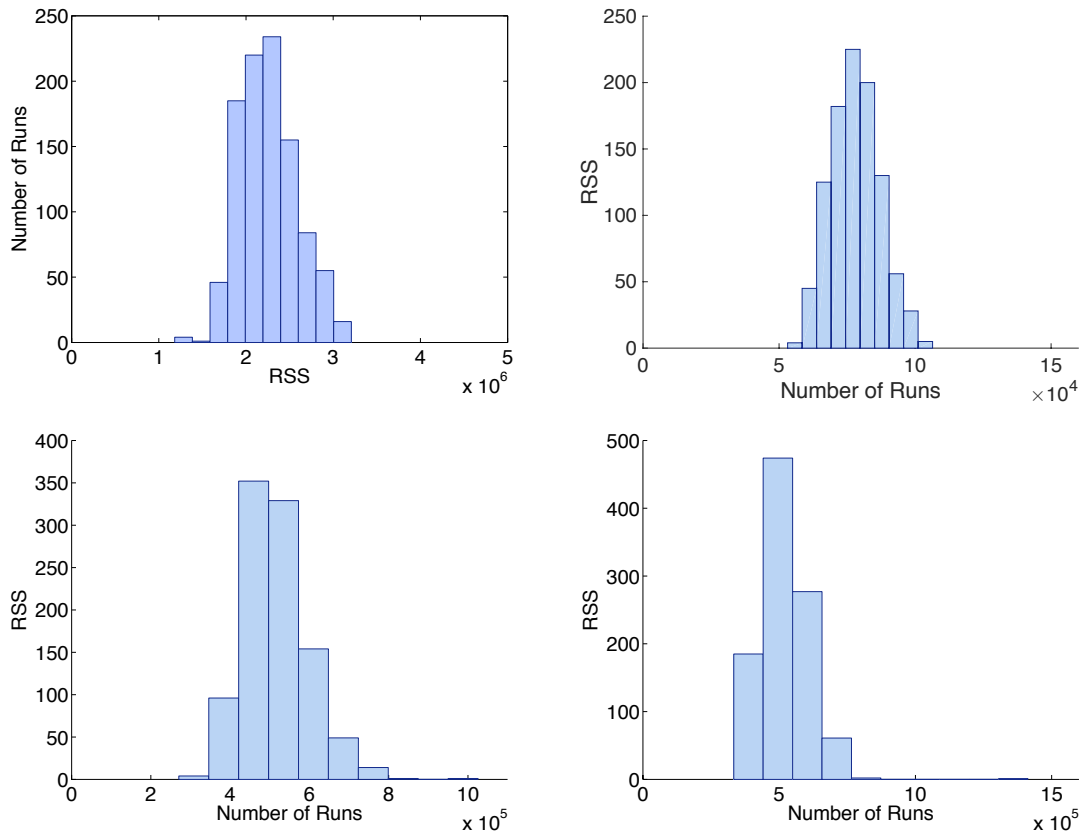


Figure 10: Histogram of residual sum of squares values for the simplified model fits to data from (left to right): all countries combined, Guinea, Liberia, and Sierra Leone (corresponding to Figure 2).

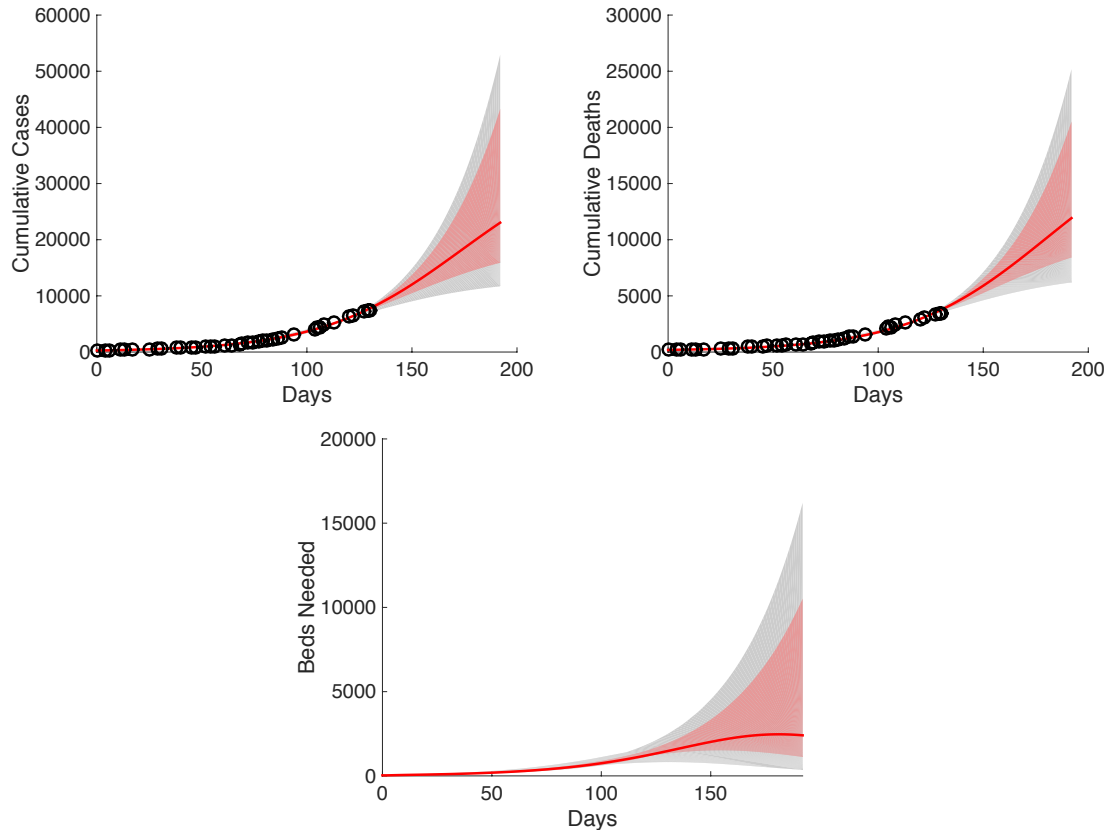


Figure 11: Model fits to data from all countries combined (as in Figure 2), with the region covered by the best 10% of all fits (lowest residual sum of squares) highlighted with red shading.

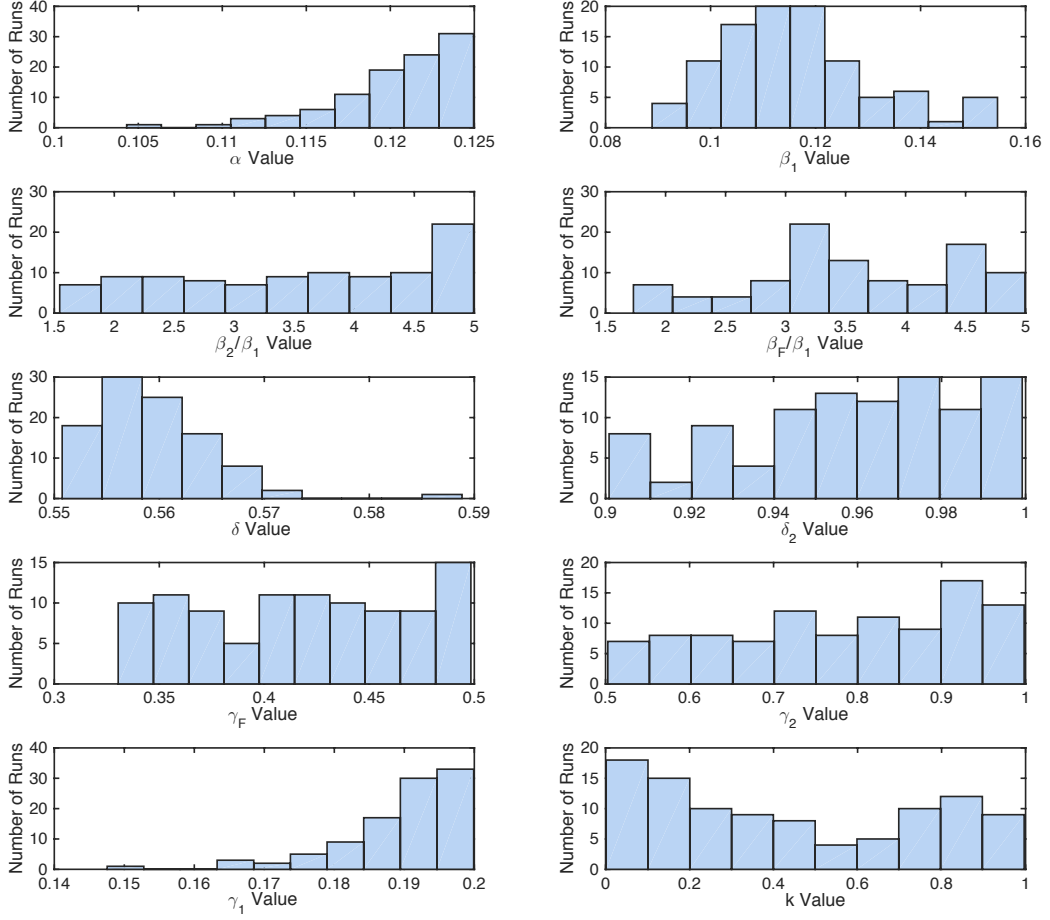


Figure 12: Histograms of parameter values from the best 10% of all fits (lowest residual sum of squares). While in some cases, the best-fit parameters tend to be clustered at a particular values, others span the full range of realistic values given in Table 1.

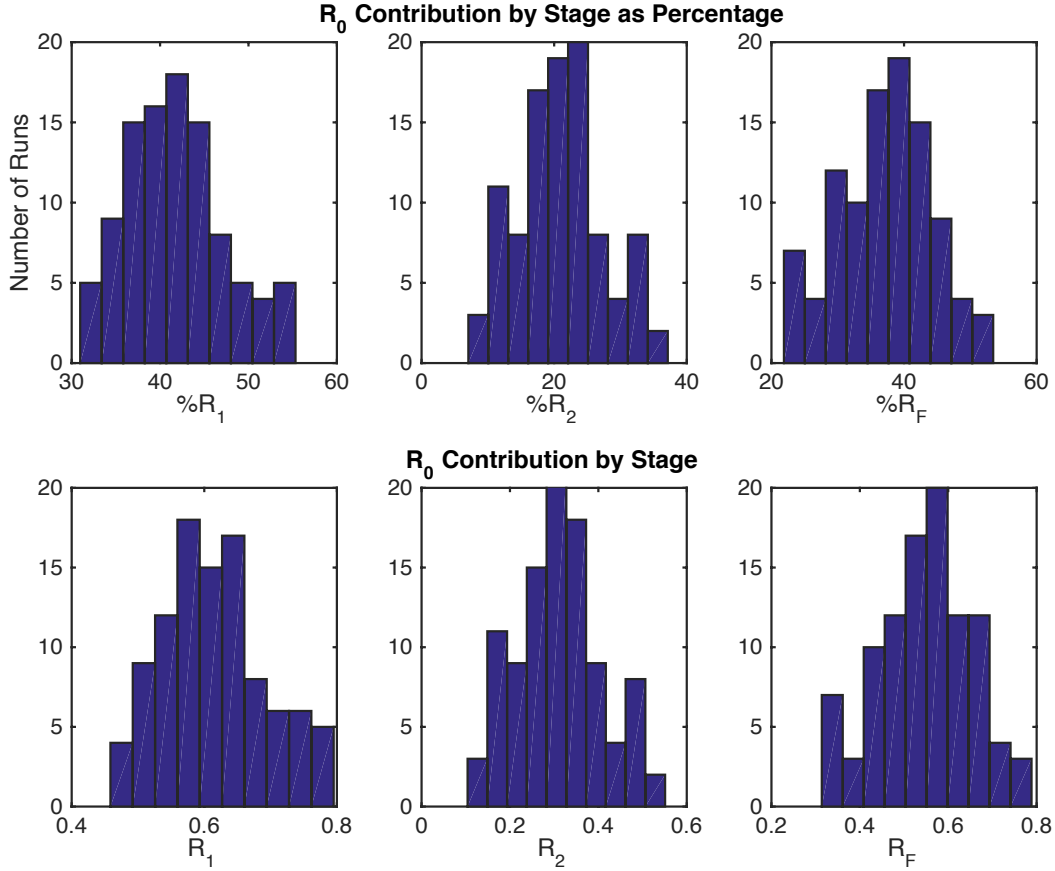


Figure 13: Histograms of \mathcal{R}_0 contributions by stage from the best 10% of all fits (lowest residual sum of squares). The top row shows contributions by stage as a percentage of overall \mathcal{R}_0 , while the bottom row shows the magnitudes of \mathcal{R}_1 , \mathcal{R}_2 , and \mathcal{R}_F (the contributions of I_1 , I_2 , and F respectively). Even among the best fit estimates, the contributions by stage to \mathcal{R}_0 span from quite low to the majority of transmission for any given stage, making it difficult to estimate the true contribution of each stage to transmission from incidence data alone.

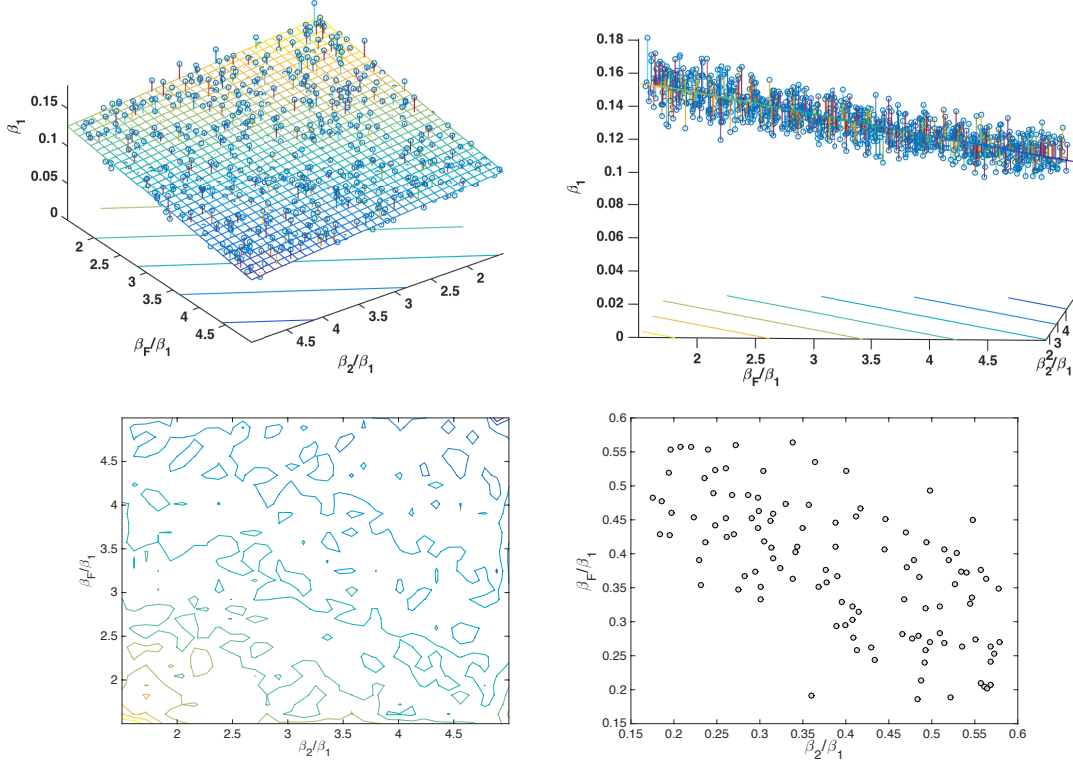


Figure 14: Top row: front (left) and side (right) views of the estimates of β_1 , β_2/β_1 , and β_F/β_1 , with the best-fit plane shown as a mesh. The three parameters have an approximately linear relationship with one another, indicating that the parameters may be unidentifiable individually, but identifiable in combination. Bottom row: left panel shows contour lines of β_2/β_1 and β_F/β_1 for fixed values of β_1 , and right panel shows a scatterplot of β_2/β_1 and β_F/β_1 for a roughly fixed value of β_1 between 0.115 and 0.12. Both panels highlight the approximately linear compensation between β_2 and β_F , such that similarly good fits can be obtained for a wide range of values, so long as the same total transmission level is maintained.